RESEARCH AND DEVELOPMENT TECHNICAL REPORT
SLCET-TR-89-7

QUARTZ CRYSTAL RESONATOR MASS LOADING

JOHN KOSINSKI
ARTHUR BALLATO
S. MALLIKARJUN (MONMOUTH COLLEGE)
ELECTRONICS TECHNOLOGY AND DEVICES LABORATORY

AUGUST 1989

US ARMY
LABORATORY COMMAND
FORT MONMOUTH, NEW JERSEY 07703-5000

UNCLASSIFIED
SECURITY CLASSIFICATION OF THIS PAGE

REPORT DOCUMENTATION PAGE

Form Approved OMB No. 0704-0188

1a. REPORT SECURITY CLASSIFICATION Unclassified	1b. RESTRICTIVE MARKINGS
2a. SECURITY CLASSIFICATION AUTHORITY	3. DISTRIBUTION/AVAILABILITY OF REPORT Approved for public release; distribution is unlimited.
2b. DECLASSIFICATION/DOWNGRADING SCHEDULE	
4. PERFORMING ORGANIZATION REPORT NUMBER(S) SLCET-TR-89-7	5. MONITORING ORGANIZATION REPORT NUMBER(S)
6a. NAME OF PERFORMING ORGANIZATION US Army Laboratory Command Electronics Tech & Devices Lab 6b. OFFICE SYMBOL (If applicable) SLCET-MA-A	7a. NAME OF MONITORING ORGANIZATION
6c. ADDRESS (City, State, and ZIP Code) Electronics Technology and Devices Laboratory ATTN: SLCET-MA Fort Monmouth, NJ 07703-5000	7b. ADDRESS (City, State, and ZIP Code)
8a. NAME OF FUNDING/SPONSORING ORGANIZATION 8b. OFFICE SYMBOL (If applicable)	9. PROCUREMENT INSTRUMENT IDENTIFICATION NUMBER
8c. ADDRESS (City, State, and ZIP Code)	10. SOURCE OF FUNDING NUMBERS PROGRAM ELEMENT NO. 1L162705 / PROJECT NO. H94 / TASK NO. K9 / WORK UNIT ACCESSION NO. DA303394

11. TITLE (Include Security Classification)
QUARTZ CRYSTAL RESONATOR MASS LOADING (U)

12. PERSONAL AUTHOR(S)
John Kosinski, Arthur Ballato, S. Mallikarjun (Monmouth College)

13a. TYPE OF REPORT	13b. TIME COVERED	14. DATE OF REPORT (Year, Month, Day)	15. PAGE COUNT
Technical Report	FROM Jan 88 TO Jun 89	1989 August	28

16. SUPPLEMENTARY NOTATION

17. COSATI CODES			18. SUBJECT TERMS (Continue on reverse if necessary and identify by block number)
FIELD	GROUP	SUB-GROUP	Piezoelectric resonators; quartz crystal plate resonators; mass loading
09	01		
17	02		

19. ABSTRACT (Continue on reverse if necessary and identify by block number)

Ongoing work aimed at determining the physical properties of cultured quartz material from frequency measurements of bulk wave resonators has highlighted the need for accurate means of measuring the mass loading due to the electrodes. In this report, various methods of determining electrode mass loading are presented, and measurements of mass loading using several of these techniques are compared. Variations between the values of mass loading obtained by the various techniques are discussed and a model is proposed to explain the various differences.

20 DISTRIBUTION/AVAILABILITY OF ABSTRACT	21. ABSTRACT SECURITY CLASSIFICATION
☐ UNCLASSIFIED/UNLIMITED ☒ SAME AS RPT. ☐ DTIC USERS	Unclassified
22a NAME OF RESPONSIBLE INDIVIDUAL John Kosinski	22b. TELEPHONE (Include Area Code) (201) 544-2843 / 22c. OFFICE SYMBOL SLCET-MA-A

DD Form 1473, JUN 86 *Previous editions are obsolete.*

SECURITY CLASSIFICATION OF THIS PAGE
UNCLASSIFIED

CONTENTS

FIGURES

TABLES

INTRODUCTION

Measurements of selected resonators are being made as part of an effort to redetermine the material properties of quartz. Preliminary results based on frequency measurements of the thickness modes of quartz plate resonators driven by thickness fields were reported in 1988 [1]. The accuracy of these results was noted as being limited by uncertainties in the values of electrode thicknesses ascribed to individual resonators. In order to resolve some of the uncertainties, a program was undertaken wherein a multiplicity of measurement methods and analysis techniques were used to determine the electrode thicknesses and resultant mass loading on a number of the samples in question. It was hoped that a satisfactory technique could be developed whereby the total electrode thickness (both sides) could be determined from a set of electrical measurements at the resonator terminals.

SIGNIFICANT EFFECTS DUE TO THE ELECTRODES

The effects associated with depositing thin metallic electrodes on the surface of a piezoelectric plate can be separated into three primary categories consisting of 1) inertial effects, 2) energy trapping effects, and 3) stress effects. If the electrodes are made sufficiently thick, wave propagation effects will also be present.

The primary inertial effect due to the electrodes is the frequency lowering commonly used as a means of frequency adjustment. To a very good approximation, the thin electrode films appear as lumped masses of mass per unit area m determined by the film density ρ_e and thickness t_e. While adding mass to the surfaces provides a convenient means of frequency adjustment, it is also a potential source of difficulty as the thermally activated transfer of contamination within a sealed resonator can easily be a significant source of frequency aging. A somewhat smaller inertial effect is an alteration of the resonator frequency-temperature behavior as the metallization thickness is varied [2,3].

Energy trapping effects are another useful result of depositing electrodes on the surface. By creating regions with different cut-off frequencies we are able to confine a large portion of the vibrational energy of a desired thickness mode to the center of the plate, greatly reducing the coupling to unwanted modes which occurs at the lateral boundaries of the plate. Through careful choice of the amount of mass loading one can achieve suppression of anharmonic modes resulting in a resonator frequency spectrum containing only the desired mode.

The effects of intrinsic stresses in the electrode films and mechanical strains due to thermal expansion mismatch of the electrode-substrate interface are somewhat smaller than the inertial and energy trapping effects, and have not to date been characterized in great detail. There are, however, both theoretical [4] and experimental [5] studies indicating that the

effects are sufficiently large as to warrant attention in the manufacture of precision resonators. Of particular interest are data by Filler [6] from which the change in the first order temperature coefficient of frequency can be calculated as a function of increasing mass loading for the case of gold electrodes on AT-cut quartz. After subtracting the inertial contribution noted previously, one finds that interfacial stresses due to the "low-stress" gold electrode contribute $+2\times10^{-7}$ per kelvin per percent of mass loading to the first order temperature coefficient of frequency. This implies that compressive stresses are being developed in the quartz at the rate of $10^4 N/m^2$ per kelvin per percent of mass loading, a value in good agreement with that calculable from the thermal expansions of gold and quartz.

ELECTRODE PROPERTIES OF INTEREST

There are a number of properties pertaining to the electrode which have an identifiable impact on resonator performance. These properties include electrical, physical, and geometric quantities.

The primary electrical characteristic of interest is the film resistivity. While it is possible to use resistivity as a tool in analyzing the physical properties of the film [7], we are generally interested only in obtaining a low resistance film so as not to degrade resonator Q.

For thin films, the physical property of most interest is the film density. The density of thin gold films as used in this paper has been reported by different authors as being between 90 percent [8] and 100 percent [9] of the bulk density value. As the film becomes thicker, the elastic properties of the film become important and the acoustic impedance of the film becomes the physical property of most interest. The combinations of film adhesion and thermal expansion (leading to interfacial strains), and intrinsic stress and surface mobility (leading to metal migration) must also be considered in certain applications.

The geometric quantities of electrode size, shape, thickness, and uniformity directly affect both the static and motional equivalent circuit parameters of a given resonance. For a given cut and blank thickness, electrode size and shape determine both static and motional capacitances, electrode thickness determines the final resonant frequency, and electrode size and uniformity determine unwanted mode content.

PIEZOELECTRIC PLATE RESONATOR

The typical piezoelectric plate resonator consisting of a quartz disk with metallic electrodes top and bottom is shown in Figure 1. The piezoelectric plate of thickness 2h and density ρ_s contains some region A_a known as the active area wherein acoustic waves are driven by voltages applied to electrodes of thickness t_e (each side) and density ρ_e. The region wherein the electrodes overlap to form a parallel plate capacitor structure is denoted as

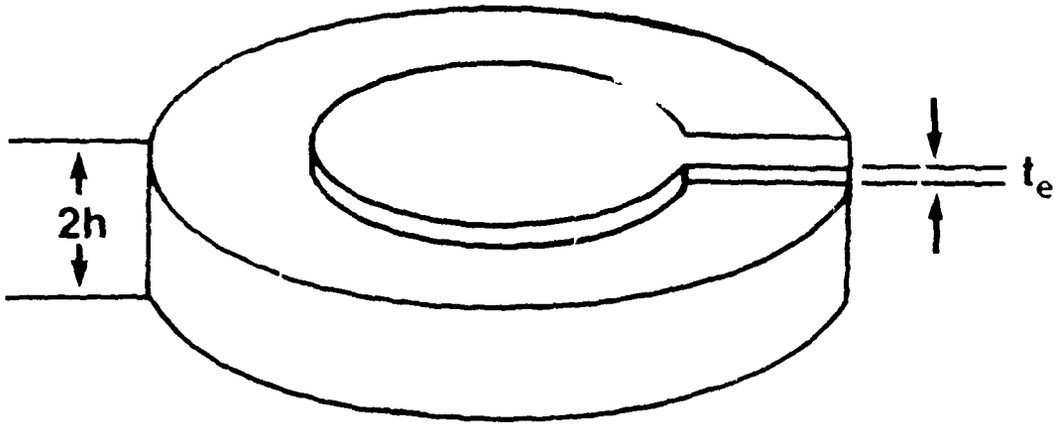

PIEZOELECTRIC PLATE:

- thickness 2h
- material properties
  ρ_s, ε_{ij}, e_{ijk}, c_{ijkl}
- active area A_a

METALLIC ELECTRODES:

- thickness t_e (each side)
- material properties
  ρ_e, Z_e, v_e
- electroded area A_e

MASS LOADING:

$$\mu = \frac{\text{electrode mass per unit area}}{\text{substrate mass per unit area}}$$

Figure 1. Piezoelectric plate resonator.

the electroded area A_e.

The inertial interaction of electrodes and substrate is conveniently described by the ratio of electrode mass per unit area to substrate mass per unit area, denoted as mass loading μ. For the case of an infinite plate with no lateral variations, the electroded and active areas are coincident and the mass loading is given by the familiar form

$$\mu = \frac{\rho_e \, t_e}{\rho_s \, h} \tag{1}$$

wherein mass loading and electrode thickness are directly proportional. The frequency perturbation resulting from a given value of mass loading can be calculated using a number of methods; this will be discussed in a subsequent section.

METHODS OF MEASURING MASS LOADING

Given that the mass loading can be calculated using (1), a means of finding the mass loading using dimensional measurements becomes apparent:

- o assume bulk properties
- o measure the unelectroded critical frequencies
- o calculate 2h
- o measure t_e
- o calculate μ

The assumption of bulk properties for the electrode film is based upon the work of Lewis and Lu [9]. The calculation of blank thickness from the unelectroded critical frequencies is well known. From a practical standpoint, this method reduces to a) being able to measure the critical frequencies of unelectroded plates, and b) being able to measure the electrode film thicknesses.

An alternative method of determining mass loading arises from the ability to calculate the mass-loading-induced frequency perturbation:

- o assume bulk properties
- o measure the unelectroded critical frequencies
- o calculate 2h
- o measure the electrode critical frequencies
- o calculate μ
- o calculate t_e

The assumption of bulk properties and the calculation of blank thickness are the same as for the dimensional measurement technique. In this case, however, we need to be able to measure the critical frequencies with and without the electrodes. In addition, the choice of equations used for calculating μ from the frequency perturbation is quite important. The assumption of

TABLE 1. THICKNESS MEASUREMENT METHODS [12]

Method	Sensitivity	Remarks
Resistance	≈1%	Convenient, empirical thickness-resistance relation required
Microbalance	≈1Å/cm^2	Simple, rate and thickness monitor
Stylus	≈20Å	Rapid, absolute, thickness and thickness profile
X-ray Emission	≈100Å	Simple, relative, thickness and thickness profile
Optical	1%	Relative, rapid, continuous scan, thickness profile
Interferometric	≈2Å	Most accurate, absolute, highly reflecting surface or overcoat required in a two-beam method where sensitivity is limited to ~50Å

lateral unboundedness is implicit in the application of (1) in both techniques. If the lateral dimensions are to be included in the treatment, the works of Tiersten [10] and Lee [11] are pertinent.

FILM THICKNESS MEASUREMENTS

There are a number of methods available for measuring the thicknesses of metallic electrodes, each with its own combination of accuracy and applicability [12]. The most common techniques are described in Table 1. In this work, we were interested in checking the actual thicknesses of films reported to us as being ≈1000Å thick. Both interferometric and stylus-type measurements were evaluated, with stylus-type measurements being chosen on the basis of greater practicality in this particular case. Sample data obtained using the stylus method are shown in Figure 2.

CRITICAL FREQUENCY MEASUREMENTS

The critical frequencies of the unelectroded piezoelectric plates were measured using an adjustable air gap fixture in conjunction with an automatic network analyzer. The resonance frequency was measured as the air gap was varied from zero to one thousand micrometers, and the data were fit by the method of least squares using the well known relationships for frequency pulling with a series load capacitor. Sample data are shown in Figure 3. Both resonance and antiresonance frequencies can be extracted from the data, which may then be converted to values of piezoelectric

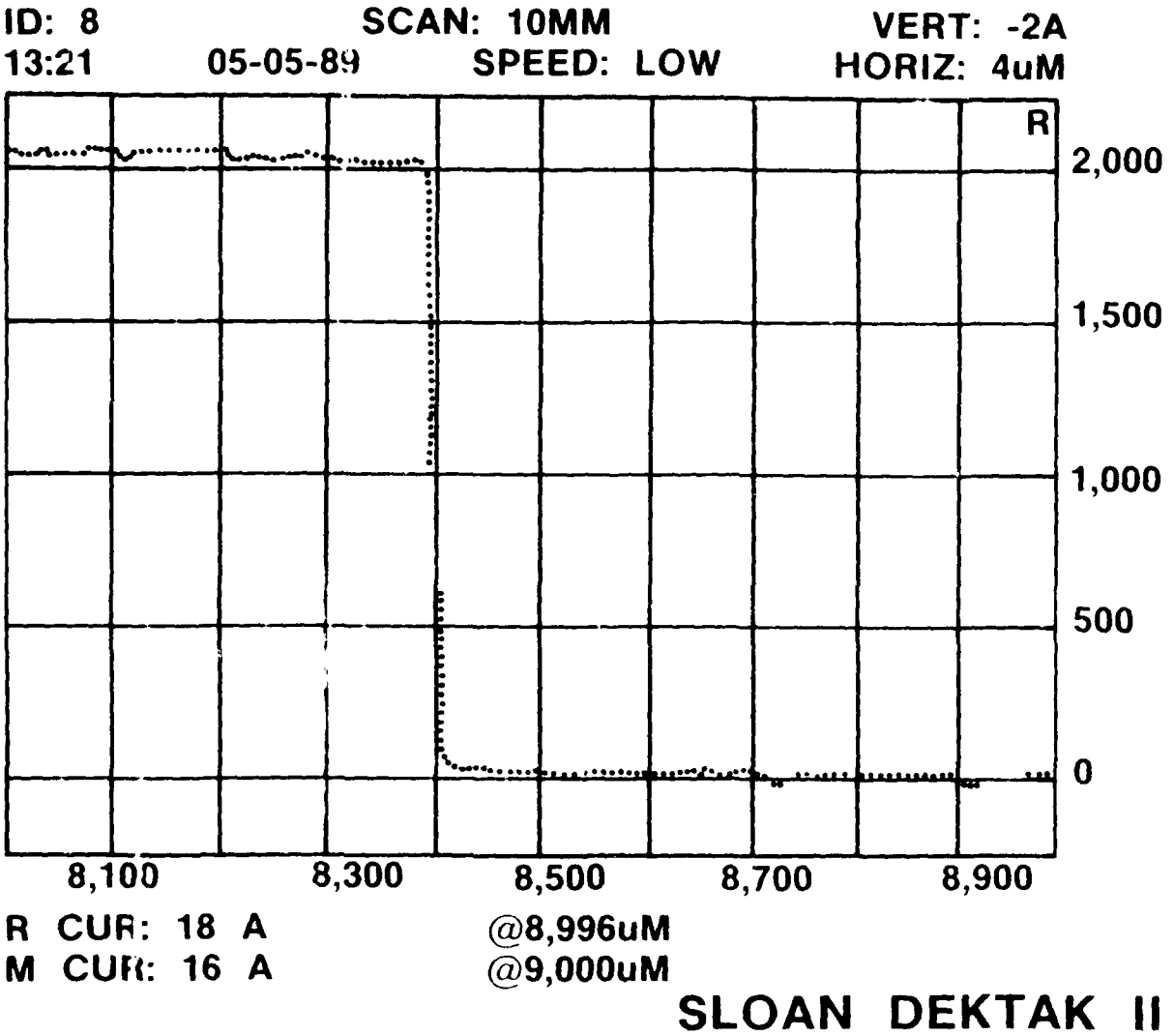

Figure 2. Sample thickness measurement data.

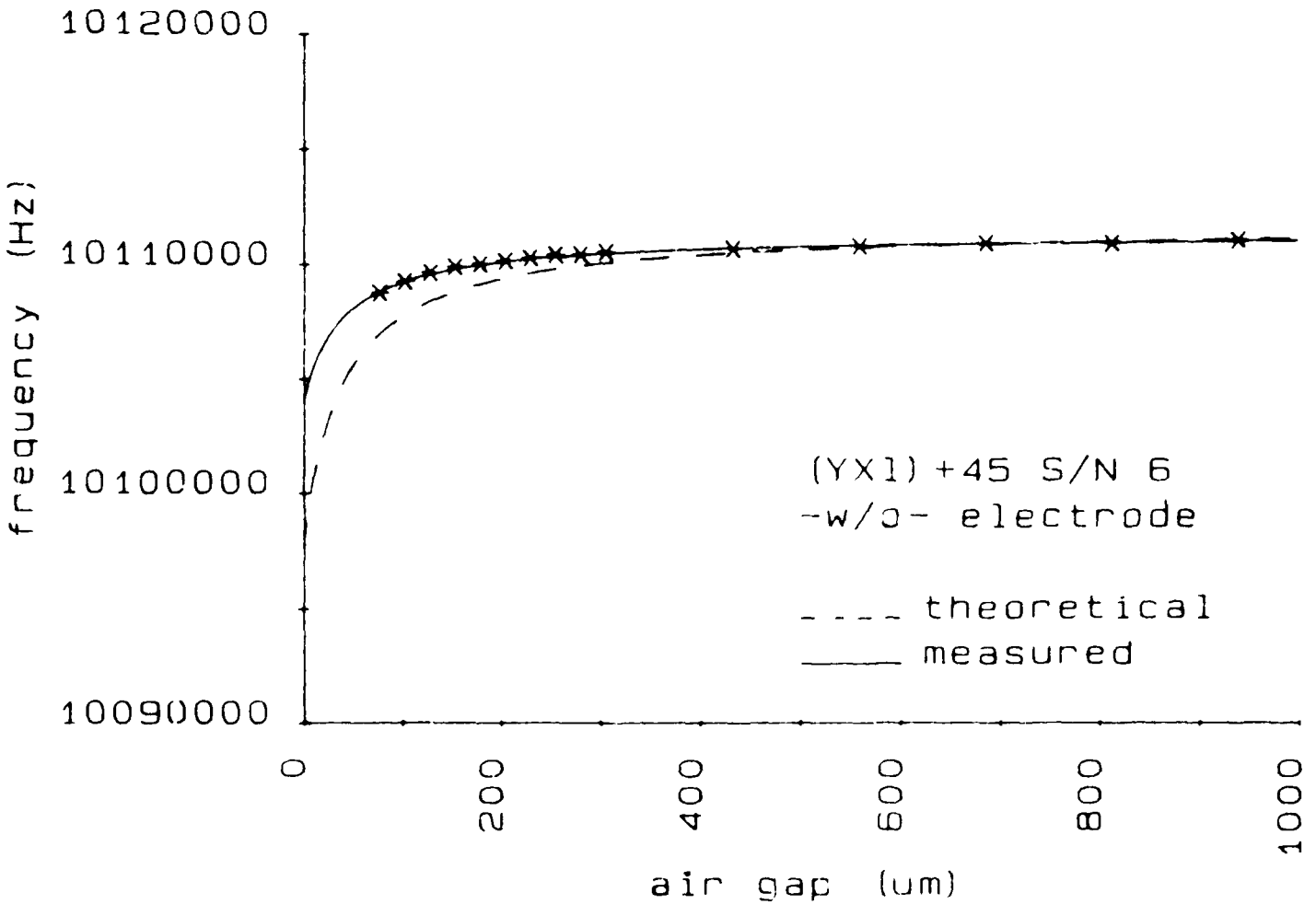

Figure 3. Sample unelectroded plate air-gap measurement data.

coupling and motional parameters.

The critical frequencies of the electroded piezoelectric plates were measured using a multiplicity of methods. Unmounted plates were measured using the same air gap fixture and analysis as described above, with the difference between resonator electrode diameter and air gap electrode diameter taken into account. Sample data are shown in Figure 4. The electroded plates were also measured while mounted and sealed in resonator enclosures. The frequency measurements were made using pi-network, impedance analyzer, network analyzer, and automatic microcircuit bridge [13] systems. Good agreement was found among all the measurement methods.

FREQUENCY MEASUREMENT ANALYSIS - MASS LOADING

A number of equation sets exist whereby the frequency perturbation due to the mass loading may be calculated with varying degrees of accuracy, with the greatest accuracy achieved through a three-dimensional equation set with non-linear piezoelectricity. For this discussion, however, we choose to employ the exact transmission line analog of a single thickness mode with no lateral variation [14], and compare these results to those obtained with two other relations commonly used to calculate mass loading.

The first investigator to formalize a relationship describing the mass loading-induced frequency perturbation was Sauerbrey [15]. The relationship, given by

$$\frac{m_e}{m_s} = - \frac{f^{(1)}_{A\mu} - f^{(1)}_{Ao}}{f^{(1)}_{Ao}} \qquad (2)$$

is considered accurate for values of mass loading up to two percent. An empirically determined constant representing film non-uniformity and lateral variations is sometimes included [16]. One should note that in (1) both m_e and m_s refer to actual masses, not areal densities.

As improvements in experimental techniques allowed thicker films to be evaluated, the relationship from Sauerbrey was modified slightly in order to extend its range of validity [17,18]. This modified relationship, known as the "period-measurement" technique, may be written as

$$\frac{m_e}{m_s} = - \frac{f^{(1)}_{A\mu} - f^{(1)}_{Ao}}{f^{(1)}_{A\mu}} \qquad (3)$$

With this small change, the relationship is considered accurate for values of mass loading up to ten percent for selected materials.

In 1968, Miller and Bolef [19] used acoustic wave analysis to calculate the shift in resonance frequencies which occurs when thin

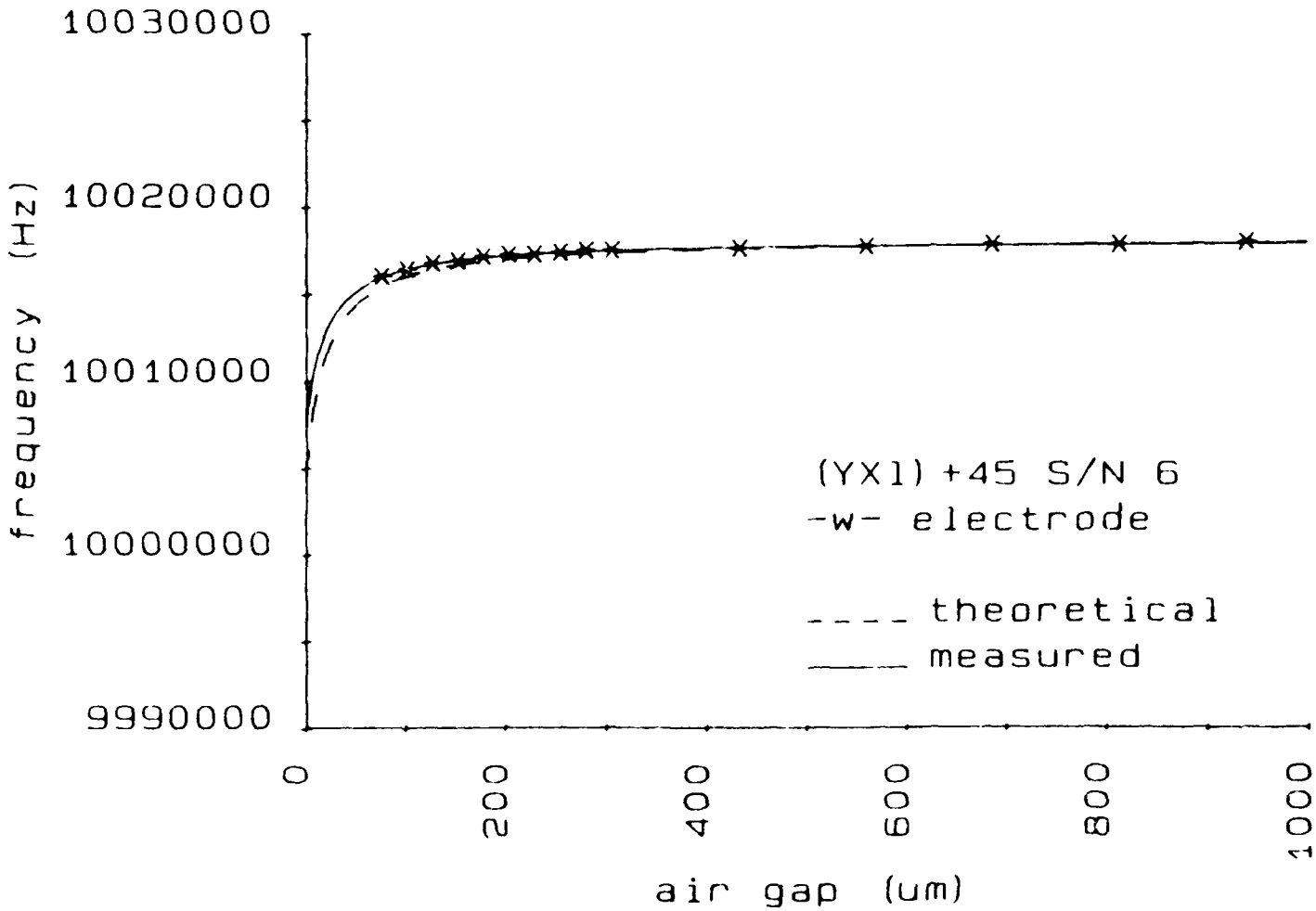

Figure 4. Sample electroded plate air-gap measurement data.

transducers are attached to an ultrasonic crystal resonator. In 1972, Lewis and Lu [20] applied the results of Miller and Bolef to the case of quartz crystal thickness monitors with large mass loading. They showed that, in the case of small losses, the frequency perturbation could be determined from

$$\frac{\rho_f v_f}{\rho_q v_q} \tan \frac{\pi f_c}{f_f} = - \tan \frac{\pi f_c}{f_q} \tag{4}$$

where v_f and v_q are the shear wave velocities in the film and quartz respectively, and ρ_f and ρ_q are the respective densities. The quantities f_f, f_q, and f_c represent the resonance frequencies of the film, the quartz substrate, and the composite resonator structure.

In 1970, Yamada and Niizeki [21] used the equations of linear piezoelectricity in conjunction with the appropriate boundary conditions to obtain expressions for the admittance of piezoelectric plate resonators. In 1972, Ballato [14] used network synthesis techniques to transform the admittance functions of Yamada and Niizeki into exact transmission line analogs of the piezoelectric plate resonator. In the case of a single mode and small mass loading, the resonance frequencies may be determined from

$$\frac{\tan X}{X} = \frac{1}{k^2 + \mu X^2}, \quad X = \frac{\pi}{2} \frac{f^{(M)}_{R\mu}}{f^{(1)}_{Ao}} \tag{5}$$

and the antiresonance frequencies may be determined from

$$\frac{\tan X}{X} = \frac{1}{\mu X^2}, \quad X = \frac{\pi}{2} \frac{f^{(M)}_{A\mu}}{f^{(1)}_{Ao}} \tag{6}$$

Equations for the case of large mass loading are simply developed using the transmission line analog, from which (4) can easily be derived. Applying (6) to the antiresonance frequencies, one can determine the mass loading directly, whereas to use (5) in conjunction with the resonance frequencies, a knowledge of the piezoelectric coupling is required.

Inasmuch as the mass loading is by definition a fixed ratio of areal densities, one should in theory be able to use the antiresonance frequencies of a series of harmonics to determine both mass loading and the unloaded fundamental antiresonance frequency. In practice, however, the situation is complicated by the non-uniform distribution of vibratory motion, so that what we measure as antiresonance is actually the point where the integral of the current density taken over the electroded area vanishes.

FREQUENCY MEASUREMENT ANALYSIS - COUPLING

As an adjunct to determining the mass loading by measuring the critical frequencies, one may also determine the effective value of piezoelectric coupling both with and without mass loading. The simplest relationship for determining the coupling is derived from the Butterworth-Van Dyke (BVD) equivalent circuit as

$$\frac{f^{(M)}_A - f^{(M)}_R}{f^{(M)}_R} = \frac{4\ k^2}{M^2\ \pi^2} \tag{7}$$

This relationship can be used both with and without mass loading in which the coupling should be denoted by k_μ or k_o respectively, with similar subscripts on the frequencies.

The transmission line analog resonance frequency equation given in (5) may also be applied either with or without mass loading. In the case of zero mass loading, (5) simplifies to

$$\frac{\tan X}{X} = \frac{1}{k^2_o}\ ,\quad X = \frac{\pi}{2}\frac{f^{(M)}_{Ro}}{f^{(1)}_{Ao}} \tag{8}$$

from which the coupling is obtained directly from the resonance frequencies, given that the fundamental antiresonance frequency is known. Inasmuch as the piezoelectric coupling for a given mode is a physical constant, one should in theory be able to use the unloaded resonance frequencies of a series of harmonics to determine both the coupling and the unloaded fundamental antiresonance frequency. If the mass loading is known, one can use (5) in conjunction with the mass loaded resonance frequencies to determine the coupling.

EXPERIMENTAL RESULTS

Frequency and film thickness measurements were performed on a number of optically polished (YXl)+38° and (YXl)-49° resonators. The resonators were 14 mm diameter, plano-plano, 10 to 14 MHz on the fundamental, with gold electrodes nominally 1000Å thick and ranging from 5.5 to 7 mm in diameter. Sample data typical of the optically polished resonators are given in Tables 2 and 3. The measured total electrode thickness $2t_e$ is compared to that obtained by combining (1) with (2), (3), and (6). The theoretical piezoelectric coupling is compared to that obtained by applying (7) to the data both with and without mass loading, by applying (5) to the mass loaded resonance frequency data using the values for mass loading obtained using (6), and by applying (8) to the unloaded resonance frequencies. A number of points concerning the mass loading are evident from the data:

1) While the mass loading is by definition a physical constant, the actual effective mass loading varies with harmonic.

2) The harmonic variations observed were consistent for a

TABLE 2. SAMPLE DATA - (YXl)+38° RESONATOR

Mass Loading (%) and Electrode Thickness (Å)

	measured	Sauerbrey		"period"		tanX/X	
M	$2t_e$	μ	$2t_e$	μ	$2t_e$	μ	$2t_e$
1	5015	1.825	4077	1.859	4153	1.860	4154
3	5015	1.914	4275	1.951	4358	1.964	4386
5	5015	1.921	4290	1.958	4374	1.981	4425
7	5015	1.916	4280	1.954	4364	1.994	4454
9	5015	1.905	4255	1.942	4338	2.003	4474

Piezoelectric Coupling (%)

	theoretical	BVD		tanX/X	
M	k	k_μ	k_o	k_μ	k_o
1	7.77	3.93	2.94	3.89	2.94
3	7.77	3.43	3.18	3.37	5.10
5	7.77	3.84	1.56	4.12	8.13
7	7.77	4.54	4.68	4.86	12.17
9	7.77	6.30	5.88	7.02	16.38

given angle of cut, but varied between different cut angles.

3) A difference between the bulk and thin film densities cannot by itself explain the mass loading data.

In order to explain the harmonic variations, it is necessary to re-examine the underlying assumptions of lateral unboundedness and a non-uniform distribution of motion.

APPROXIMATIONS FOR FINITE ELECTRODES - BVD EQUIVALENT CIRCUIT

Bechmann [22] is generally credited with being the first to model the effects of a non-uniform distribution of motion on the fully electroded piezoelectric plate resonator. He introduced a factor Psi equal to the quotient of the square of the surface integral of the normalized amplitude function (proportional to the electrical energy) divided by the surface integral of its square

TABLE 3. SAMPLE DATA - (YXl)-49° RESONATOR

Mass Loading (%) and Electrode Thickness (Å)

	measured		Sauerbrey		"period"		tanX/X	
M	$2t_e$	μ	$2t_e$	μ	$2t_e$	μ	$2t_e$
1	3500	1.305	2325	1.322	2355	1.322	2349
3	3500	1.311	2336	1.329	2367	1.325	2354
5	3500	1.308	2329	1.325	2360	1.318	2344
7	3500	1.316	2344	1.333	2376	1.346	2418

Piezoelectric Coupling (%)

	theoretical	BVD		tanX/X	
M	k	k_μ	k_o	k_μ	k_o
1	5.66	3.45	3.55	3.43	3.55
3	5.66	3.22	3.64	3.20	1.52
5	5.66	3.22	2.92	3.21	--
7	5.66	3.30	4.69	3.31	8.02

(proportional to the mechanical energy). Denoting the plate area as A and the amplitude distribution function as f(x,z), we have

$$\Psi = \frac{\left[\frac{1}{A} \int f(x,z)\ dA \right]^2}{\frac{1}{A} \int f^2(x,z)\ dA} \qquad (9)$$

Psi, which is always less than or equal to one, is used as a multiplier in calculating the motional capacitance of the BVD equivalent circuit and as a divisor in calculating the motional inductance and resistance. In Bechmann's treatment of partially electroded plates, the integral in the numerator is taken over the electroded area and the resultant expression multiplied by the electroded fraction of the total plate area.

Building on the work of Bechmann, Sauerbrey [23] added a correction for the inhomogeneous boundary field at the edge of the

electrode. The influence of the boundary field is simulated by extending the area of integration by an amount equal to the fraction of static capacitance arising from the fringing field. The modified Psi is then given by

$$\Psi = \frac{A'}{A}\,\frac{A'}{A_e}\,\frac{\left[\frac{1}{A'}\int f(x,z)\,dA'\right]^2}{\frac{1}{A}\int f^2(x,z)\,dA} \tag{10}$$

where A' represents the extended area. The influence of the boundary field leads to a non-negligible increase in the distribution factor and corresponding changes in the motional parameters.

APPROXIMATIONS FOR FINITE ELECTRODES - TRANSMISSION LINE ANALOG

The transmission line analog for a single piezoelectrically driven mode, in the case of thick electrode films, is shown in Figure 5. Implicit in the derivation of this equivalent circuit are the assumptions of lateral unboundedness and a uniform distribution of motion. A simple first approximation to the practical case of lateral boundedness can be made by retaining the assumption of a uniform distribution of motion but allowing for a difference between the electroded area A_e and the active area A_a. The equivalent circuit elements are then calculated as

$$C_o = \frac{\epsilon\, A_e}{2h} \tag{11}$$

$$N = \frac{e\, A_a}{2h} \tag{12}$$

$$Z = A\,\rho\, v \tag{13}$$

$$k = \frac{2\,\pi\, f}{v} \tag{14}$$

It is also expedient to introduce the concept of the electroded fraction of the active area, here denoted b. The natural upper bound of b = 1 is approached in the work of Lewis and Lu [9]. Since b is always less than or equal to 1, b is conveniently expressed as a percentage. For the common case of equal size electrodes as encountered here, $b = A_e / A_a$.

EFFECTIVE COUPLING AND MASS LOADING

If one employs (9) thru (12) in finding the critical

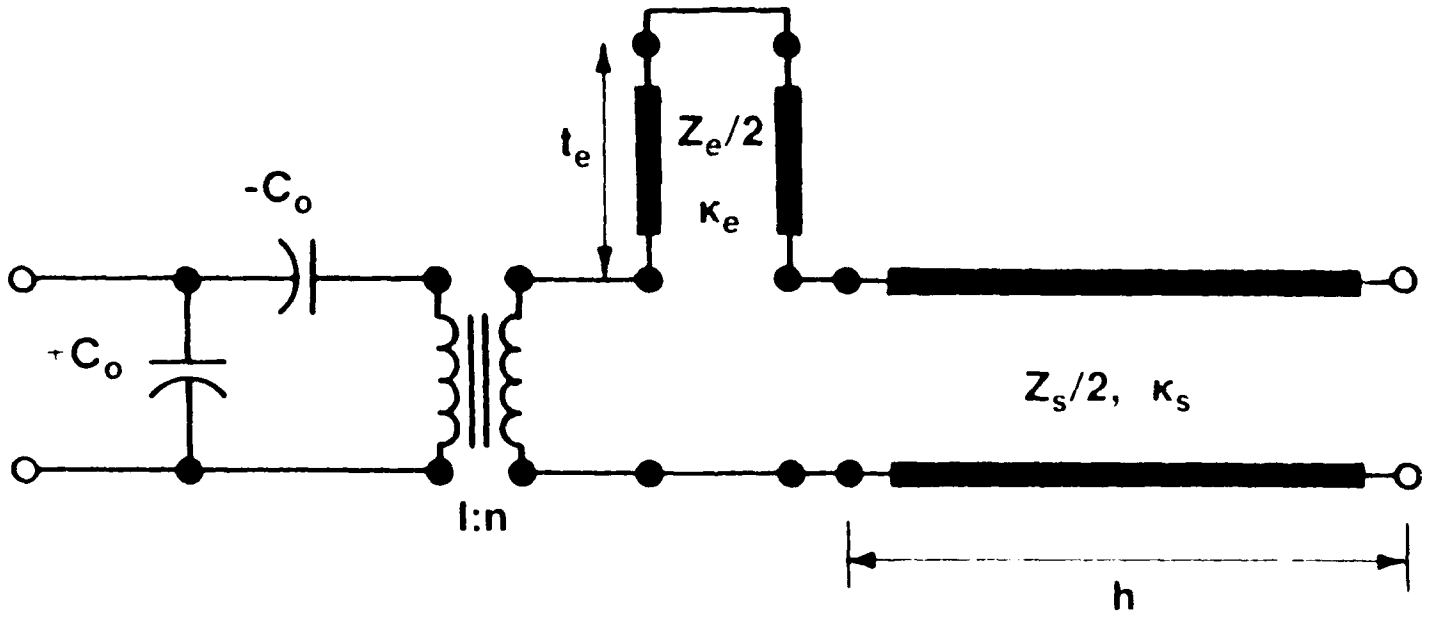

Figure 5. Transmission line analog for a single TETM mode, bisected basis.

frequencies of the transmission line analog of Figure 5, one obtains equations (5) and (6) with the difference that the piezoelectric coupling k and mass loading μ are now replaced by effective values k_{eff} and μ_{eff}. The effective coupling is given by

$$k^2_{eff} = \frac{k^2}{b} \tag{15}$$

and the effective mass loading is given by

$$\mu_{eff} = \mu\ b\ \frac{\tan X_e}{X_e} \tag{16}$$

The effective mass loading is seen to be the product of the "ideal case" mass loading for thin films given by (1), the electroded fraction of the active area b, and a transcendental term relating to wave propagation in the case of thick films. The term X_e is defined similarly to the X of equations (5) and (6), being equal to one-half pi times the ratio of the critical frequency being measured to the fundamental antiresonance frequency of the total electrode film of thickness $2t_e$.

One can readily solve for the electrode thickness required for the "onset" of wave propagation effects by setting the term $(\tan X_e/X_e)$ equal to the sum of unity plus some maximum allowable perturbation level. Figure 6 shows the relationship between the maximum allowable perturbation level and the minimum required ratio Ω between the fundamental antiresonance frequency of the electrodes (based on the total electrode thickness, both sides included) and the critical frequency of interest of the mass loaded resonator. The maximium allowable electrode thickness t_{max} (each side) corresponding to a maximum allowable perturbation level can be found by using Figure 6 in conjunction with

$$t_{max} = \frac{v}{4\ \Omega\ f_c} \tag{17}$$

TABLE 4. SELECTED WAVE VELOCITIES (m/sec) [24]

Material	Shear Wave Velocity	Longitudinal Wave Velocity
Al	3040	6420
Cu	≈2300	≈4900
Au	1200	3240
Mo	3350	6250
Ni	≈3000	≈5750
Ag	1610	3650
W	≈2750	≈5300

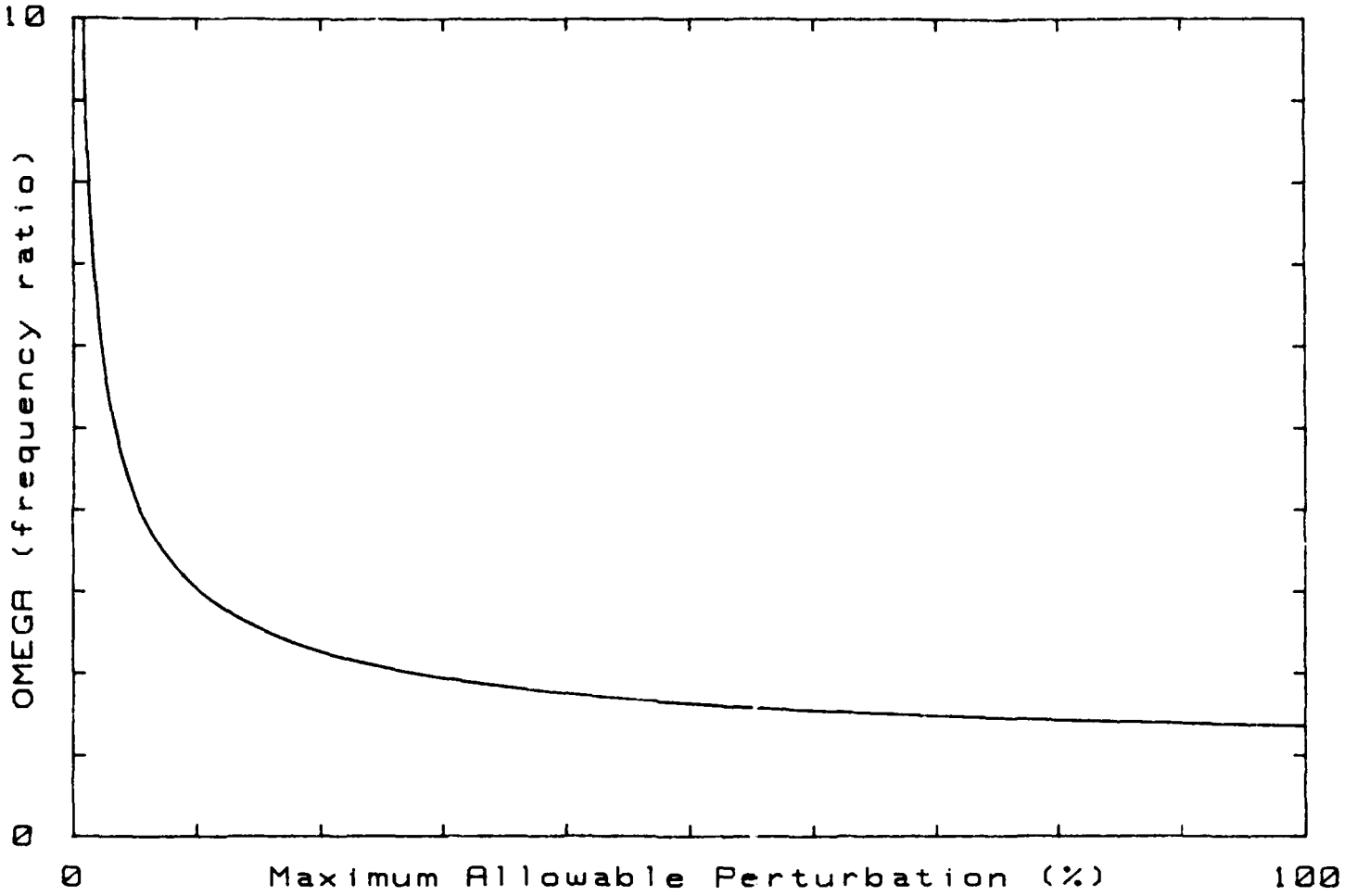

Figure 6. Minimum required electrode to resonator frequency ratio Ω versus maximum allowable effective mass loading perturbation due to thick electrodes.

TABLE 5. ELECTRODED FRACTION OF THE ACTIVE AREA

M	(YXl)+38°	(YXl)-49°
1	82.8%	67.1%
3	87.5%	67.3%
5	88.2%	67.0%
7	88.8%	69.1%
9	89.2%	--

where v is the appropriate wave velocity in the electrode film. Acoustic wave velocities for some common electrode materials are listed in Table 4 [24]. Applying (17) to the case of 10 MHz thickness-shear resonators with gold electrodes, one finds that 33000Å thick electrodes (each side) are required to cause a one percent perturbation in the effective mass loading.

ANALOGY TO BECHMANN'S NUMBER

Table 5 lists typical data for the areal ratio b observed as a function of angle of cut and harmonic of operation. The data for (YXl)+38° are in good agreement with the areal ratio b=88.3% calculated using the expressions for the effective length of the motional volume of partially electroded AT-cut resonators as given by Sykes and Beaver [25].

For comparison, the harmonic dependence of the energy trapping criterion known as Bechmann's Number is shown in Figures 7 and 8 for the case of AT and BT-cuts respectively [26]. The trend toward better energy trapping with increasing harmonic number for the AT-cut case compares nicely to the increasing electroded fraction of the active area with increasing harmonic number as shown by the data. For the BT-cut, the more complex energy-trapping-harmonic relationship is also well mirrored, as is the overall fact that the AT-cut energy traps much better than the BT-cut.

CONCLUSIONS

Measurements have been made of the electrode thicknesses and resultant mass loadings on a number of piezoelectric plate resonators. Significant differences have been found between the theoretical and effective mass loading, including variations in the effective mass loading measured for different harmonics. A simple first approximation to the effects of lateral boundedness which provides qualitative insights as to the cause of the variations has been presented.

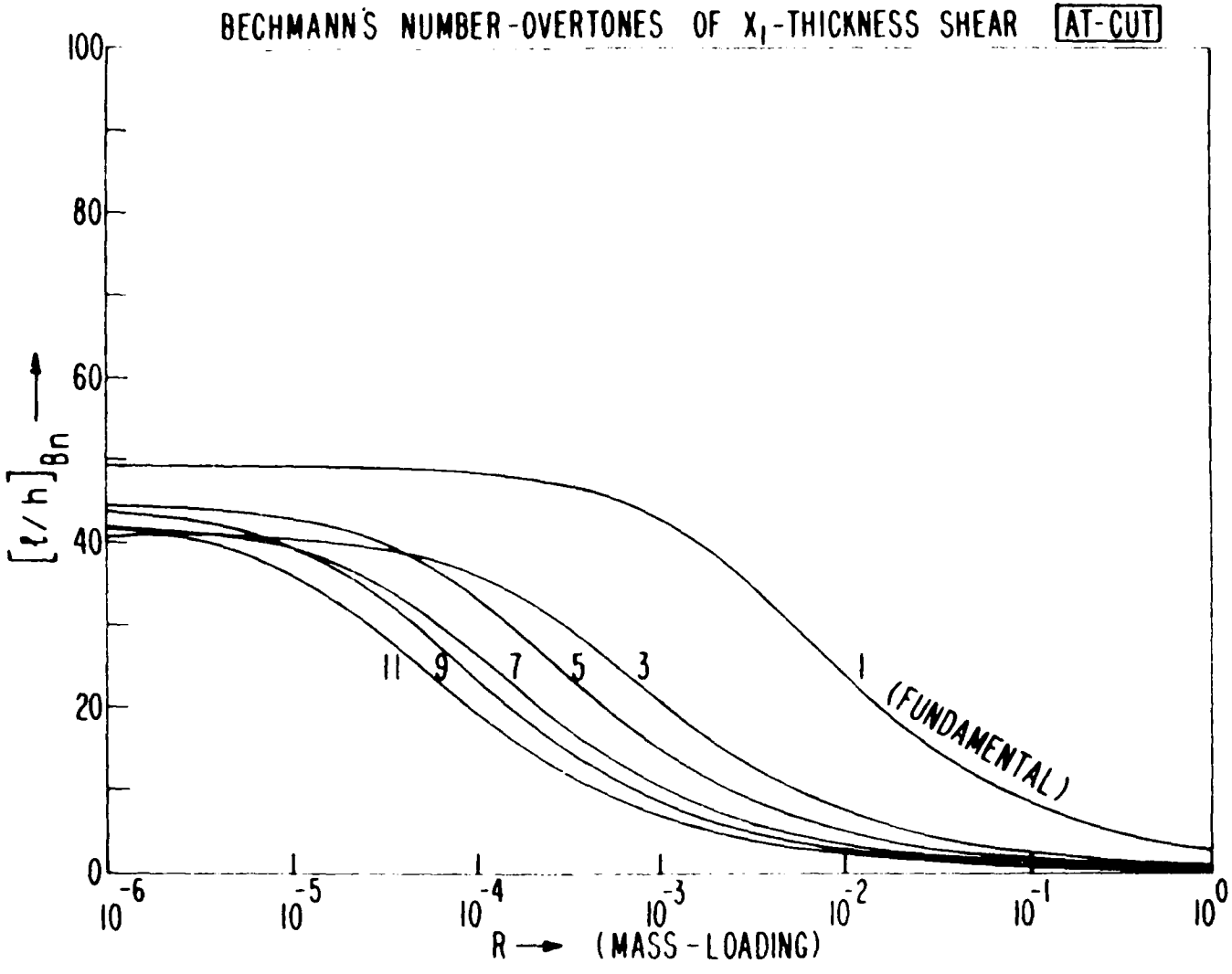

Figure 7. Bechmann's Number for the AT-cut.

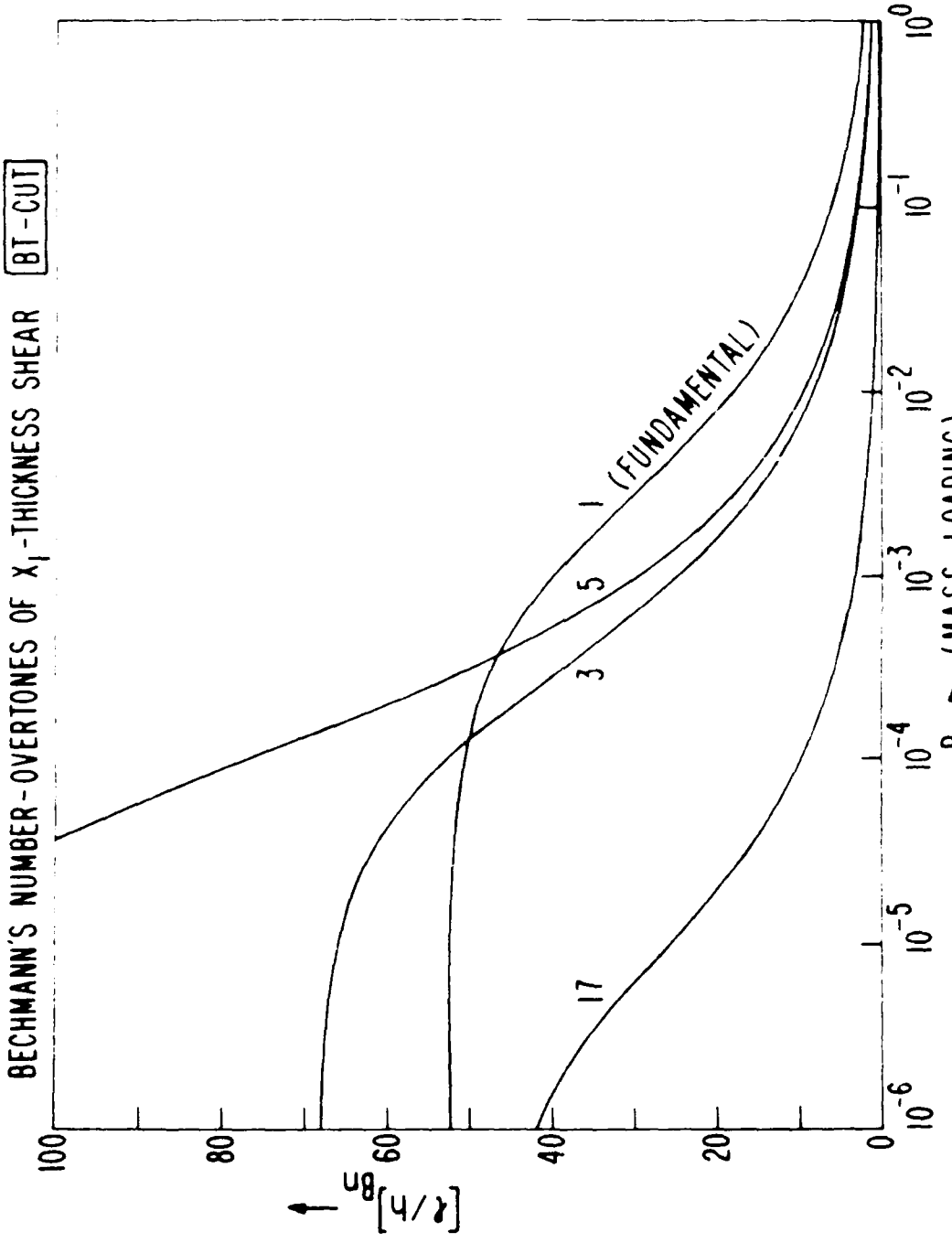

Figure 8. Bechmann's Number for the BT-cut.

REFERENCES

[1] J. Kosinski, A. Ballato, T. Lukaszek, M. Mizan, R. McGowan, and K. Klohn, "Temperature Derivatives of the Dynamic Permittivity and Permeability of the Simple Thickness Modes of Quartz Plates," Proc. 42nd Annual Frequency Control Symposium, pp. 53-64, June 1988.

[2] A. Ballato and T. Lukaszek, "Higher Order Temperature Coefficients of Frequency of Mass Loaded Piezoelectric Crystal Plates," Proc. 29th Annual Frequency Control Symposium, pp. 10-25, May 1978.

[3] A. Ballato, T. J. Lukaszek, and G. J. Iafrate, "Subtle Effects in High Stability Vibrators," Proc. 34th Annual Frequency Control Symposium, pp. 431-444, May 1980.

[4] E. P. EerNisse, "Quartz Resonator Frequency Shifts Arising From Electrode Stress," Proc. 29th Annual Frequency Control Symposium, pp. 1-4, May 1975.

[5] J. H. Sherman, "Temperature Coefficient of the Frequency Shift Arising from Electrode Film Stress," IEEE Trans. on Sonics and Ultrasonics, Vol. 30, No. 2, pp. 104-110, March 1983.

[6] R. L. Filler and J. R. Vig, "Fundamental Mode SC-cut Resonators," Proc. 34th Annual Frequency Control Symposium, pp. 187-193, May 1980.

[7] L. Maissel and R. Glang, eds. Handbook of Thin Film Technology. New York:McGraw-Hill, 1970.

[8] E. P. EerNisse, private communication, May 1989.

[9] O. Lewis and C. Lu, "Relationship of Resonant Frequency of Quartz Crystal to Mass Loading," Proc. 29th Annual Frequency Control Symposium, pp. 5-9, May 1975.

[10] D. S. Stevens and H. F. Tiersten, "An Analysis of Doubly-Rotated Contoured Quartz Crystal Resonators," Proc. 39th Annual Frequency Control Symposium, pp. 436-447, May 1985.

[11] P. C. Y. Lee and M. S. H. Tang, "Initial Stress Field and Resonance Frequencies of Incremental Vibrations in Crystal Resonators by Finite Element Method," Proc. 40th Annual Frequency Control Symposium, pp. 152-160, May 1986.

[12] K. L. Chopra, Thin Film Phenomena. New York:McGraw-Hill, 1969, pp. 83-136.

[13] E. Hafner, "QXMS-1M Automatic Crystal Measurement System," XOTEX Corp., P. O. Box 1026, Eatontown, N. J. 07724, 1989, 2 pp.

[14] A. D. Ballato, "Transmission Line Analogs for Stacked

Piezoelectric Crystal Devices," Proc. 26th Annual Frequency Control Symposium, pp. 86-91, June 1972.

[15] G. Z. Sauerbrey, "Verwendung von Schwingungen zur Wägung dünner Schichten und zur Mikrowägung," Zeitschrift der Physik, Vol. 155, p. 206, 1959.

[16] C. D. Stockbridge, "Resonance Frequency Versus Mass Added to Quartz Crystals," in Vacuum Microbalance Techniques, Vol. 5 (K. Behrdt, ed.). New York:Plenum Press, 1966, pp. 193-205.

[17] K. H. Behrndt, "Long-Term Operation of Crystal Oscillators in Thin-Film Deposition," Journal of Vacuum Science and Technology, Vol. 8, No. 5, pp. 622-626, September 1971.

[18] D. R. Denison, "Linearity of a Heavily Loaded Quartz Crystal Microbalance," Journal of Vacuum Science and Technology, Vol. 10, No. 1, pp. 126-129, January 1973.

[19] J. G. Miller and D. I. Bolef, "Sensitivity Enhancement by the Use of Acoustic Resonators in cw Ultrasonic Spectroscopy," Journal of Applied Physics, Vol. 39, No. 10, pp. 4589-4593, September 1968.

[20] C. Lu and O. Lewis, "Investigation of Film-Thickness Determination by Oscillating Quartz Resonators With Large Mass Load," Journal of Applied Physics, Vol. 43, No. 11, pp. 4385-4390, November 1972.

[21] T. Yamada and N. Niizeki, "Admittance of Piezoelectric Plates Under Perpendicular Field Excitation," Proc. of the IEEE, Vol. 58, No. 6, pp. 941-942, June 1970.

[22] R. Bechmann, "Uber Dickenschwingungen piezoelektrischer Kristallplatten," Archiv. der elekr. Ubertragung, Vol. 6, pp. 361-368, 1952.

[23] G. Sauerbrey, "Amplitudenverteilung und elektrische Ersatzdaten von Schwingquarzplatten (AT-Schnitt)," Archiv. der elekr. Ubertragung, Vol. 18, pp. 624-628, 1964.

[24] R. Weast, ed., CRC Handbook of Chemistry and Physics, 49th Ed.. Cleveland:Chemical Rubber Co., 1968, p. E38.

[25] R. Sykes and W. Beaver, "High Frequency Monolithic Crystal Filters With Possible Application to Single Frequency and Single Side Band Use," Proc. 20th Annual Frequency Control Symposium, pp. 288-308, April 1966.

[26] H. F. Tiersten, "Analysis of Trapped Energy Resonators Operating in Overtones of Thickness-Shear," Proc. 28th Annual Frequency Control Symposium, pp. 44-48, May 1974.

ELECTRONICS TECHNOLOGY AND DEVICES LABORATORY
MANDATORY DISTRIBUTION LIST
CONTRACT OR IN-HOUSE TECHNICAL REPORTS

101 Defense Technical Information Center*
ATTN: DTIC-FDAC
Cameron Station (Bldg 5)
Alexandria, VA 22304-6145

(*Note: Two copies for DTIC will be sent from STINFO Office.)

483 Director
US Army Material Systems Analysis Actv
ATTN: DRXSY-MP
001 Aberdeen Proving Ground, MD 21005

563 Commander, AMC
ATTN: AMCDE-SC
5001 Eisenhower Ave.
001 Alexandria, VA 22333-0001

609 Commander, LABCOM
ATTN: AMSLC-CG, CD, CS (In turn)
2800 Powder Mill Road
001 Adelphi, Md 20783-1145

612 Commander, LABCOM
ATTN: AMSLC-CT
2800 Powder Mill Road
001 Adelphi, MD 20783-1145

680 Commander,
US Army Laboratory Command
Fort Monmouth, NJ 07703-5000
1 - SLCET-DD
2 - SLCET-DT (M. Howard)
1 - SLCET-DB
35 - Originating Office

681 Commander, CECOM
R&D Technical Library
Fort Monmouth, NJ 07703-5000
1 - ASQNC-ELC-I-T (Tech Library)
3 - ASQNC-ELC-I-T (STINFO)

705 Advisory Group on Electron Devices
201 Varick Street, 9th Floor
002 New York, NY 10014-4877